Depinning transition of a pattern forming system in a washboard potential

Jeenu Kim* and Jysoo Lee†
Supercomputing Research Department, Korea Institute of Science and Technology Information, Daejeon 305-806, Korea
(Received 19 March 2004; published 26 July 2004)

We investigate numerically the depinning transition of the Kuramoto-Sivashinsky equation in a washboard potential in one dimension, and find three distinct behaviors. For a certain range of parameters, the transition is well described by the mean field exponent of 1/2. The next case is that the critical behavior is dominated by the growth of spatially periodic mode with critical exponent 1. Finally, a parameter range exists in which intermittent movement is observed. "Anchor," which is a spontaneously generated coherent structure, acts as a pinning center. The destruction of anchor is shown to involve a topological change of "unknotting."

DOI: 10.1103/PhysRevE.70.016213 PACS number(s): 05.45.Xt, 47.20.Ky, 89.75.Kd

Pattern formation in the nonequilibrium system is widely observed in many physical, chemical, and biological systems, and has been the subject of many studies for a few decades [1]. One of the current issues is the effect of external perturbation on a pattern forming system. Frequently, such a system interacts with its surrounding, and understanding the effect of extrinsic perturbation is of great theoretical and practical importance. Examples of such systems include light sensitive Belousov-Zhabotinsky reaction, catalytic oxidation on metal surface, and array of chaotic electrochemical oscillators [2]. Various spatiotemporal patterns observed in these experiments and their theoretical models have been studied extensively [3–5].

It is often the case that such systems follow external forcing for sufficiently large forcing amplitude. In the "moving" frame of the forcing, the systems are "pinned." As the forcing amplitude decreases, deviation from the motion of the forcing starts to appear, and the system become "depinned." Although depinning is a prominent feature of many forced pattern forming systems, we are not aware of any quantitative study on the transition. Also, the depinning transition is related to the synchronization among coupled chaotic oscillators [6].

In this paper, we study numerically the depinning transition of a one-dimensional phase equation derived from forced complex Ginzburg-Landau equation (CGLE) around 1:1 locking. The phase equation is essentially the Kuramoto-Sivashinsky equation [7] in a washboard potential. Depending on parameters, three distinct transition behaviors are observed. First is a mean field behavior. For a certain range of parameters, spatial modulation plays no role, and the transition is well described by the mean field exponent of $\theta=1/2$. The exponent θ is defined by $\Omega \sim \epsilon^{\theta}$, where ϵ is the reduced forcing amplitude and Ω is the rotation rate, which is equal to the average velocity of phase. The next case is that the critical behavior is dominated by the growth of unstable modes with finite wavelength. An approximate expression for the growth rate is obtained, and it predicts θ to be 1, which is in excellent agreement with numerical simulations. Finally, there exist a parameter region within which intermittent movement is observed. "Anchor," which is one of coherent structures spontaneously generated, plays a key role as a pinning center near the transition. In four-dimensional phase space, anchor has the structure of a knot, and its destruction involves a topological change of "unknotting."

The complex Ginzburg-Landau equation (CGLE) is the universal amplitude equation for the class of systems where the bifurcation at the onset of a pattern is supercritical and oscillatory, and the most unstable wavenumber is zero [1,8]. When a sinusoidal forcing is added, it was shown that an additional term should be included, which can be determined from the conditions of spatial and temporal translation invariance [3]. Near 1:1 resonance, the resulting equation is

$$\partial_t A = (1+i\nu)A - (1+i\alpha)|A|^2 A + (1+i\beta)\nabla^2 A + \gamma, \quad (1)$$

in the reference frame of the forcing. Here, $A(x,t)$ is complex amplitude describing slow modulation of uniform oscillation. The forcing is represented by dimensionless forcing frequency ν and forcing amplitude γ. The real constant α is related to nonlinear frequency shift, and β is to relative dispersion [1,8].

An approximate phase equation can be derived from Eq. (1) using the assumption that R follows adiabatically ϕ, where $A=\mathrm{Re}^{i\phi}$ [9]. The resulting equation is

$$\partial_t \phi = \omega - B \sin\phi + b(\partial_x \phi)^2 + c\partial_x^2 \phi + d\partial_x^4 \phi, \quad (2)$$

where $\omega=\nu-\alpha$, $B=\gamma\sqrt{1+a^2}$, and a,b,c, and d are constants given by $a=\alpha-\omega/2$, $b=\alpha-\beta-\omega/2$, $c=1+\alpha\beta-\beta\omega/2$, and $d=-\beta^2/2$. The biharmonic term $(\partial_x^4\phi)$ is present to ensure the stability of solution when the harmonic term is destabilizing due to negative c. Compared to the Kuramoto-Sivashinsky (KS) equation [7], two additional terms are present in the equation: (1) constant drift ω due to frequency mismatch, and (2) harmonic "force" term $B\sin\phi$. In other words, the effect of the external forcing is to add a washboard potential $V(\phi)=-\omega\phi-B\cos\phi$ to the KS equation. The drift term tries to move the phase in one direction, while the harmonic term tends to pin such a movement. The KS equation has a wide range of applications from chemical wave to ion sputtering, and is central in the study of spatiotemporal chaos in extended systems [7]. Equation (2) is

*Electronic address: lontano@kisti.re.kr
†Electronic address: jysoo@kisti.re.kr

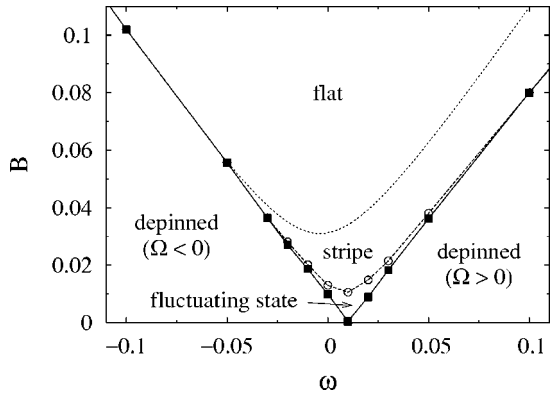

FIG. 1. The stability borders of the "flat" state B_f (dotted line) and the "stripe" state B_s (○) for the phase equation Eq. (2) with $\alpha=-3/4$ and $\beta=2$ are shown. Also shown is the depinning threshold line B_d (■).

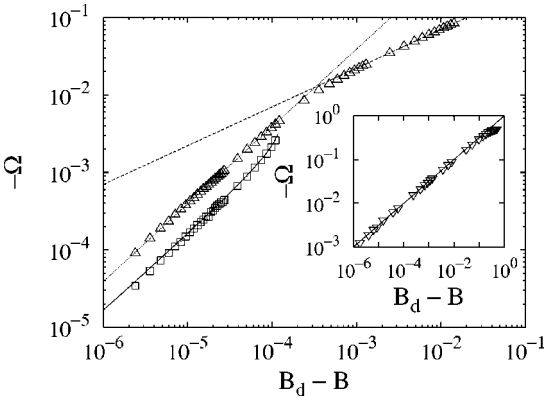

FIG. 2. Log–log plot of $-\Omega$ vs (B_d-B) at $\omega=-0.25$ ($B_d=0.250\,122$). Data from numerical integration (triangles) is shown, along with a linear (dotted line) and square root (dashed line) behavior. Measured growth rate of the amplitude of the stripe state (squares) and predictions from a linear stability analysis (solid line) are also plotted. Shown in the inset is the B dependence of Ω for $\omega=\omega_c=-0.5$ ($B_d=0.5$), which is well fitted by a square root function.

expected to show generic features of the systems in which pattern forming instability, periodic potential, and driving force are competing with each other. Therefore, the phase equation is also important irrespective of its relation to the forced CGLE.

The unforced system is characterized by two parameters—α and β. The effect of the forcing has been studied for several combinations of α and β, and more interesting case of Benjamin-Feir unstable region $(1+\alpha\beta<0)$ will be reported here [8]. Defect, a point in space with $|A|=0$, is present in the amplitude turbulence part of the region, and the phase equation can no longer be a good approximation of the original Eq. (1). The case of $\alpha=-3/4$, $\beta=2$, which is in the phase turbulence regime, will be mainly discussed throughout this letter. Although defect is absent in the regime for the CGLE, it can still appear in a forced CGLE [4]. We have also studied numerically the depinning transition of the original forced CGLE Eq. (1). Indeed, a few differences from the phase equation have been found. However, many of the results to be discussed later, including the mean field and mode growth dominated behaviors, are also observed. The full description on the results of the forced CGLE and phase equation will be published elsewhere [10].

Equation (2) has one stable homogeneous ("flat") solution in $[0,2\pi)$ interval, which is stable against uniform perturbation, only when B is larger than $|\omega|$. A linear stability analysis shows that the flat state is linearly stable when B is larger than stability border B_f, where the wavenumber of the most unstable mode k_0 is $\sqrt{-c/2d}$ for $c\leqslant 0$, and is zero otherwise. As B becomes smaller than B_f, stationary periodic pattern ("stripe") with wavelength $2\pi/k_0$ appears through a supercritical bifurcation [9]. As B decreases further (below B_s), the stripe state becomes no longer stable, and starts to fluctuate in time. As B decreases even further below B_d, average phase has a nonzero drift. Define rotation rate Ω by $\lim_{t\to\infty}[\langle\phi(x,t)\rangle-\langle\phi(x,0)\rangle]/t$, where $\langle\cdots\rangle$ denotes spatial average. The rotation rate is zero for $B>B_d$ (the system is "pinned"), and becomes nonzero below B_d ("depinned"). Three borders—B_f, B_s, and B_d—are shown in Fig. 1.

Mean field approximation of Eq. (2) is obtained by ignoring the terms involving spatial derivative:

$$\dot{\phi}=\omega-B\sin\phi. \tag{3}$$

For $B\geqslant|\omega|$, there exist a stable fixed point at which the system is pinned. For $B<|\omega|$, the average phase moves with time, and it is easy to show that the magnitude of rotation rate Ω is given by $\sqrt{\omega^2-B^2}$. Here, depinning occurs at $B_d=|\omega|$ as a result of a saddle node bifurcation. The depinning transition is characterized by critical exponent θ defined by $\Omega\sim(B_d-B)^\theta$, and θ for the mean field equation is $1/2$. In general, mean field approximation is crude, but it will describe the critical behavior well if spatial modulation is negligible. Consider again the linear stability of the flat state. The wavenumber of the most unstable mode k_0 is zero for $c>0$, which is equivalent to $\omega<\omega_c=2(1+\alpha\beta)/\beta=-1/2$. It can also be shown that B_f coincides with B_d if $k_0=0$. These facts imply that spatial modulation can be ignored near the transition for $\omega\leqslant\omega_c$, which is confirmed by numerical integration. The mean field exponent of $\theta=1/2$ is clearly demonstrated as shown in the inset of Fig. 2.

When ω is above, but remains close to ω_c ($\omega_c<\omega\lesssim-0.03$), a different transition behavior is observed. Figure 2 shows the dependence of Ω on B for $\omega=-0.25$. Away from the transition point B_d, the data are well described by the square root behavior of the mean field solution. As B approaches B_d, however, the system crosses over to a linear behavior of $\theta=1$. The time evolution of the average phase $\langle\phi\rangle$ and the fluctuation of the phase $\delta\phi\equiv\sqrt{\langle\phi^2\rangle-\langle\phi\rangle^2}$ for $\omega=-0.05$ near the transition is shown in Fig. 3. After an initial transient, the motion is very regular. It consists of "growth stage" of duration τ_g and "jump stage" of duration τ_j. At the beginning of the growth stage [marked as (a) in Fig. 3], the phase field is nearly homogeneous. As the amplitude of unstable modes grow exponentially, which increases $\delta\phi$ [(b) in Fig. 3], part of the system approaches the unstable homogeneous solution. After crossing it, two fronts rapidly propagating in opposite directions appear [curve (c)

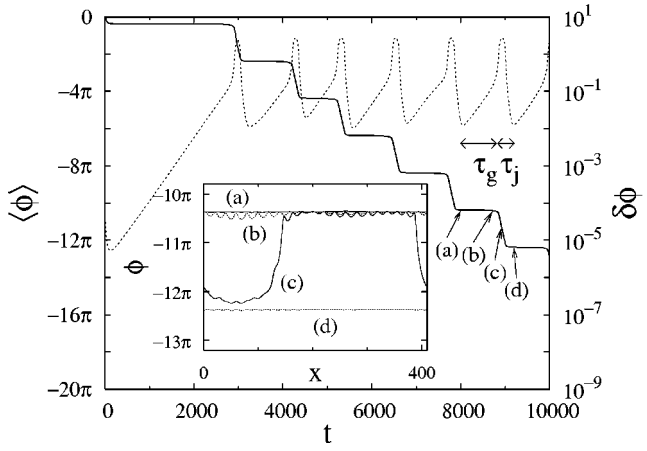

FIG. 3. Time evolutions of average phase (solid line, left axis) and spatial fluctuation of phase (dotted line, right axis) are shown for $\omega=-0.05$ and $B=0.054\,35$. The motions are almost periodic. Shown in the inset are four selected snapshots of the phase field.

in the inset]. They annihilate after colliding with each other, leaving the phase field nearly homogeneous like (a) with $\langle\phi\rangle$ decreased by 2π [curve (d)]. Then the process is repeated.

Since the average phase decreases by 2π during the period of $\tau_g+\tau_j$, rotation rate Ω is $-2\pi/(\tau_g+\tau_j)$. The time of τ_g increases, and diverges as B approaches B_d, while τ_j remains finite. Note also that τ_g is inversely proportional to the growth rate σ of the most unstable mode. Combining both, we obtain $\Omega=-2\pi/(\tau_g+\tau_j)\approx-2\pi/\tau_g\sim-\sigma$. Since the depinning transition point B_d is very close to the stability border B_f of the flat state, σ can be approximated by $\sigma_{\max}$—the growth rate of the most unstable mode near B_f. In Fig. 2, measured values of σ for $\omega=-0.25$ are shown along with $\sigma_{\max}$, where the agreement between the two are clear. By expanding $\sigma_{\max}$ around B_d, one obtains $\sigma_{\max}\sim(B_d-B)$, implying $\theta=1$.

A completely different depinning transition behavior is observed for $\omega\gtrsim0.1$. Rotation rate Ω in the regime is much smaller than that of the mean field theory, and the motion is very irregular. Shown in Fig. 4(a) is the time evolution of average phase $\langle\phi\rangle$. The most notable feature is the presence of "plateau" of various length, making the evolution intermittent. Near the transition, the average length of the plateau becomes long and dominates time evolution. Faceting, which nearly spans the whole system, is always observed at plateau [Fig. 4(b)]. Once such a large facet is formed, the field translates in the x direction while almost preserving its shape [e.g., compare Eqs. (2) and (3)], resulting no change of $\langle\phi\rangle$. Eventually, the facet becomes unstable (4), followed by relatively fast advance of $\langle\phi\rangle$, until a new system wide facet is formed. The intermittent behavior shown in Fig. 4 is similar to that in the synchronization of coupled chaotic oscillators [6].

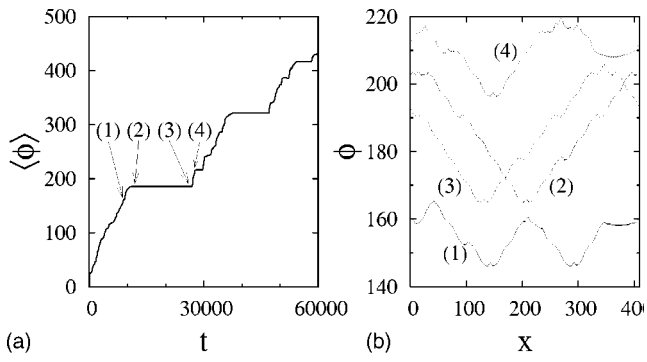

FIG. 4. (a) Irregular time evolution of average phase at $\omega=0.25$ and $B=0.1972$, where a system wide facet is present at each plateau, (b) four snapshots of the phase field before (1) and after (4), and during (2) and (3) a plateau.

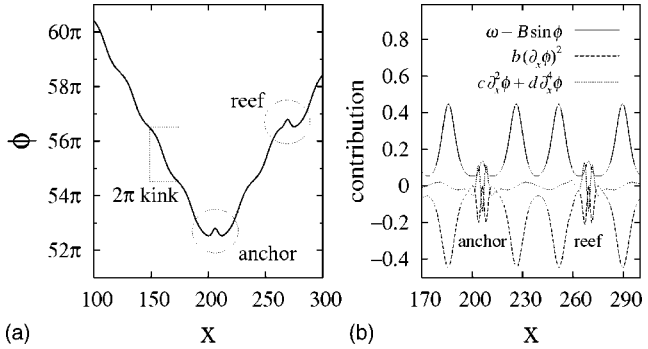

FIG. 5. (a) A system wide facet, at $\omega=0.25$ and $B=0.1972$ where 2π kinks are connected by coherent structures such as anchor and reef. (b) Contribution to the phase equation is divided into three parts: potential term $\omega-B\sin\phi$, nonlinear term $b(\partial_x\phi)^2$, and linear derivative term $c\partial_x^2\phi+d\partial_x^4\phi$.

Next, the mechanism for the faceting will be discussed. Start with the observation that a few local structures frequently appear near the transition. Two of them—"anchor" and "reef"—are displayed in Fig. 5(a). A coherent structure is a solution of the form $f(x-vt)$ for a suitable choice of f and v [11]. It is found that both anchor and reef are coherent structures based on 25 independent simulations using different values of ω, B, and initial condition: no significant evolution in shape is observed. The measured velocity v is very small, and no selection mechanism is apparent. For the parameter region of the present discussion ($\omega\gtrsim0.1$), the system is spatially periodic with significant amplitude of modulation near the transition. As B decreases below B_d, a pair of 2π kinks can be created by fluctuation, and they can propagate and annihilate upon collision. Here, anchor plays a particularly important role. Once formed, it is quite stable, and acts as a strongly pinned site. Since another part of the system advances by creation and annihilation of kinks, the span of the phase field increases, resulting in a system wide facet.

The stability of anchor can be understood by dividing the terms in the phase Eq. (2) into three parts: (1) potential term of $\omega-B\sin\phi$, (2) nonlinear term of $b(\partial_x\phi)^2$; and (3) linear derivative term of $c\partial_x^2\phi+d\partial_x^4\phi$. The contributions of these terms around coherent structures with $\omega=0.25$ and $B=0.1972$ are shown in Fig. 5(b). One of the main features is that the linear derivative term is relatively small except near the center of anchor or reef, and the potential term and nonlinear term are almost identical except their sign. The balance between the two makes an anchor stable to small fluctuations: If the slope of an anchor increases by deformation,

the contribution of the nonlinear term increases while that of the potential term is not much changed. As a result, the slope of the kinks around the anchor decreases, restoring the anchor to the original shape. Similar restoring mechanism is applied when the slope of an anchor is decreased.

Collapse of a system wide facet is always initiated by destruction of the anchor. Fluctuations near an anchor induces small deformations which is fast decaying. However, large deformation can appear, and the local slope of the two local minima in the anchor can be reduced significantly enough that the nonlinear term is negligible. Then the potential term becomes dominant, and pulls up the curve.

Additional insights can be obtained by studying anchor in a phase space. For a coherent structure, Eq. (2) can be rewritten as a set of four coupled first order differential equations $d\phi/dx=\phi'$, $d\phi'/dx=\phi''$, $d\phi''/dx=\phi'''$, $d\phi'''/dx=-[\omega - B\sin\phi - b(\phi')^2 + c\phi'']/d$, for the variables of ϕ, ϕ', ϕ'', and ϕ'''. In Fig. 6, a sequence of images for the destruction of an anchor is shown in a three dimensional projection of the phase space. An anchor prior to collapse is shown in (a). The main "loop" corresponds to the double minimum of the anchor, and the two rings at the end are 2π kinks around it. The lines extending from the rings cross at top, resulting in a knotted structure. The pretzel-like structure of (a) can be regarded as an open ended-trefoil knot, a well known structure in knot theory [12]. The destruction of anchor is initiated by a large perturbation which makes one half of the loop to expand outward and pass a ring (b), which is equivalent to the deformation and destruction of the left local minimum in Fig. 5(a). The resulting single loop (c) then simply stretches itself, completing the destruction process (d). The fact that removing an anchor involves a topological change can explain its stability: the amplitude of the perturbation should be large enough to change its topological structure. The structure of anchor near the transition is studied with varying ω. It is found that the knotted topological structure is preserved, but the radius of the main loop decreases with decreasing ω, which makes it less stable. No stable anchor is observed for $\omega \lesssim 0.1$ [10].

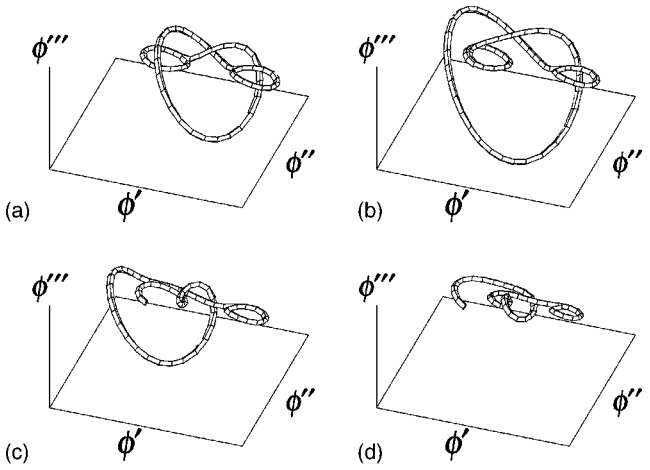

FIG. 6. Time evolution of the destruction of an anchor in a three-dimensional projection (ϕ', ϕ'', ϕ''') of the four-dimensional phase space with at $\omega=0.25$ and $B=0.1972$. Note that the pretzel shaped knot is untied.

We have studied the depinning transition of the Kuramoto-Sivashinsky equation in a washboard potential, and have found three distinct regimes: (1) mean field, (2) regime which is determined by the most unstable mode, and (3) intermittent growth regime. Compared to the first two, understanding of the last regime is largely qualitative, and more quantitative study is strongly desired.

This work is supported in part by the Korea Science and Engineering Foundation through R01-2002-000-00038-0(2002) and research fund from IBM Korea.

[1] See, e.g., M. C. Cross and P. C. Hohenberg, Rev. Mod. Phys. **65**, 851 (1993).

[2] V. K. Vanag *et al.*, Nature (London) **406**, 389 (2000); M. Kim *et al.*, Science **292**, 1357 (2001); W. Wang, I. Z. Kiss, and J. L. Hudson, Phys. Rev. Lett. **86**, 4954 (2001); K. Martinez *et al.*, Physica D **168-169**, 1 (2002).

[3] P. Coullet and K. Emilsson, Physica D **61**, 119 (1992).

[4] D. Walgraef, *Spatio-Temporal Pattern Formation* (Springer, New York, 1997); C. Elphick, A. Hagberg, and E. Meron, Phys. Rev. Lett. **80**, 5007 (1998); H. Chaté, A. Pikovsky, and O. Rudzick, Physica D **131**, 17 (1999); H.-K. Park, Phys. Rev. Lett. **86**, 1130 (2001); R. Gallego *et al.*, Phys. Rev. E **64**, 056218 (2001); C. Hemming and R. Kapral, Physica A **306**, 199 (2002).

[5] O. Steinbock, V. Zykov, and S. C. Müller, Nature (London) **366**, 322 (1993); A. L. Lin *et al.*, Phys. Rev. Lett. **84**, 4240 (2000).

[6] A. Pikovsky, M. Rosenblum, and J. Kurths, *Synchronization* (Cambridge University Press, Cambridge, UK, 2001); S. Boccaletti, *et al.* Phys. Rep. **366**, 1 (2002).

[7] Y. Kuramoto and T. Tsuzuki, Prog. Theor. Phys. **55**, 356 (1976); G. I. Sivashinsky, Acta Astron. **6**, 569 (1979); Y. Kuramoto, *Chemical Oscillations, Waves and Turbulence* (Springer, Berlin, 1984).

[8] I. S. Aranson and L. Kramer, Rev. Mod. Phys. **74**, 99 (2002).

[9] J. Kim, J. Lee, and B. Kahng, Phys. Rev. E **65**, 046208 (2002).

[10] J. Kim and J. Lee (unpublished).

[11] W. van Saarloos and P. C. Hohenberg, Physica D **56**, 303 (1992).

[12] W. B. R. Lickorish, *An Introduction to Knot Theory* (Springer, New York, 1997).